inhibitor and employs a novel mechanism. DYYRK also inhibited the autophosphorylation of IR, suggesting that it employs the same mechanism as DIYET. Moreover, the potent inhibitory effect of NIYQT is not negligible, although the peptide is an ATP-competitive inhibitor. More studies on these peptides could lead to the development of a novel peptidic drug.

REFERENCES

1. Schlessinger J. Cell signaling by receptor tyrosine kinases. *Cell* 2000; **103**: 211–225.
2. Blume-Jensen P, Hunter T. Oncogenic kinase signaling. *Nature* 2001; **411**: 355–365.
3. Al-Obeidi A, Wu1 JJ, Lam KS. Protein tyrosine kinases: structure, substrate specificity, and drug discovery. *Biopolymers* 1998; **47**: 197–223.
4. Levitzki A, Gazit A. Tyrosine kinase inhibition: an approach to drug development. *Science* 1995; **267**: 1782–1788.
5. Lee J, Pilch PF. The insulin receptor: structure, function, and signaling. *Am. J. Physiol.* 1994; **266**: C319–C334.
6. White MF, Shoelson SE, Keutmann H, Kahn CR. A cascade of tyrosine autophosphorylation in the β-subunit activates the phosphotransferase of the insulin receptor. *J. Biol. Chem.* 1988; **263**: 2969–2980.
7. Skolnik EY, Batzer A, Li N, Lee C-H, Lowenstein E, Mohammadi M, Margolis B, Schlessinger J. The function of GRB2 in linking the insulin receptor to Ras signaling pathways. *Science* 1993; **260**: 1953–1955.
8. Saltiel AR, Kahn CR. Insulin signaling and the regulation of glucose and lipid metabolism. *Nature* 2001; **414**: 799–806.
9. Hubbard SR, Mohammadi M, Schlessinger J. Autoregulatory mechanisms in protein-tyrosine kinases. *J. Biol. Chem.* 1998; **273**: 11987–11990.
10. Shewchuk LM, Hassell AM, Ellis B, Holmes WD, Davis R, Horne EL, Kadwell SH, McKee DD, Moore JT. Structure of the Tie2 RTK domain: self-inhibition by the nucleotide binding loop, activation loop, and C-terminal tail. *Structure* 2000; **8**: 1105–1113.
11. Chiara F, Bishayee S, Heldin C-H, Demoulin J-B. Autoinhibition of the platelet-derived growth factor beta-receptor tyrosine kinase by its C-terminal tail. *J. Biol. Chem.* 2004; **279**: 19732–19738.
12. Meyer RD, Singh AJ, Rahimi N. The carboxyl terminus controls ligand-dependent activation of VEGFR-2 and its signaling. *J. Biol. Chem.* 2004; **279**: 735–742.
13. Yokoyama N, Ischenko I, Hayman MJ, Miller WT. The C terminus of RON tyrosine kinase plays autoinhibitory role. *J. Biol. Chem.* 2005; **280**: 8893–8900.
14. Wybenga-Groot LE, Baskin B, Ong SH, Tong J, Pawson T, Sicheri F. Structural basis for

autoinhibition of the Ephb2 receptor tyrosine kinase by the unphosphorylated juxtamembrane region. *Cell* 2001; **106**: 745–757.

15. Hubbard SR, Wei L, Ellis L, Hendrickson WA. Crystal structure of the tyrosine kinase domain of the human insulin receptor. *Nature* 1994; **372**: 746–754.
16. Hubbard SR. Crystal structure of the activated insulin receptor tyrosine kinase in complex with peptide substrate and ATP analog. *EMBO J.* 1997; **16**: 5572–5581.
17. Ablooglu AJ, Frankel M, Rusinova E, Ross JBA, Kohanski RA. Multiple activation loop conformations and thier regulatory properties in the insulin receptor's kinase domain. *J. Biol. Chem.* 2001; **276**: 46933–46940.
18. Hirose M, Kuroda Y, Sawa S, Nakagawa T, Hirata M, Sakaguchi M, Tanaka Y. Suppression of insulin signalling by a synthetic peptide KIFMK suggests the cytoplasmic linker between DIII-S6 and DIV-S1 as a local anaesthetic binding site on the sodium channel. *Br. J. Pharmacol.* 2004; **142**: 222–228.
19. Berman HM, Westbrook J, Feng Z, Gilliland G, Bhat TN, Weissig H, Shindyalov IN, Bourne PE. The Protein Data Bank. *Nucleic Acids Res.* 2000; **28**: 235–242.
20. DeLano WL. PyMOL: an open-source molecular graphics tool. *PPC4 Newsl. Prot. Crystallogr.* 2002; **40**: 11.
21. Pettersen EF, Goddard TD, Huang CC, Couch GS, Greenblatt DM, Meng EC, Ferrin TE. UCSF Chimera–a visualization system for exploratory research and analysis. *J. Comput. Chem.* 2004; **25**: 1605–1612.
22. Cornell WD, Cieplak P, Bayly CI, Gould IR, Merz KM Jr, Ferguson DM, Spellmeyer DC, Fox T, Caldwell JW, Kollman PA. A second generation force field for the simulation of proteins, nucleic acids, and organic molecules. *J. Am. Chem. Soc.* 1995; **117**: 5179–5197.
23. Kuntz ID. Structure-based strategies for drug design and discovery. *Science* 1992; **257**: 1078–1082.
24. Kuntz ID, Meng EC, Shoichet BK. Structure-Based Molecular Design. *Acc. Chem. Res.* 1994; **27**: 117–123.
25. Shoichet BK, Bodian DL, Kuntz ID. Molecular docking using shape descriptors. *J. Comput. Chem.* 1992; **13**: 380–397.
26. Meng EC, Shoichet BK, Kuntz ID. Automated docking with grid-based energy evaluation. *J. Comput. Chem.* 1992; **13**: 505–524.
27. Ewing TJA, Makino S, Skillman AG, Kuntz ID. DOCK4.0: search strategies for automated molecular docking of flexible molecule databases. *J. Comput. Aided. Mol. Des.* 2001; **15**: 411–428.
28. Kollman PA, Massova I, Reyes C, Kuhn B, Huo S, Chong L, Lee M, Lee T, Duan Y, Wang W, Donini O, Cieplak P, Srinivasan J, Case DA, Cheatham TE III. Calculating structures and free energies of complex molecules: combining molecular mechanics and continuum models. *Acc. Chem. Res.* 2000; **33**: 889–897.
29. Onufriev A, Bashford D, Case DA. Exploring protein native states and large-scale conformational changes with a modified generalized born model. *Proteins* 2004; **55**: 383–394.

30. Mills JEJ, Dean PM. Three-dimensional hydrogen-bond geometry and probability information from a crystal survey. *J. Comput. Aided. Mol. Des.* 1996; **10**: 607–622.

31. Ward WH, Cook PN, Slater AM, Davies DH, Holdgate GA, Green LR. Epidermal growth factor receptor tyrosine kinase: ivestigation of catalytic mechanism, structure-based searching and discovery of a potent inhibitor. *Biochem. Pharmacol.* 1994; **48**: 659-666.

32. Paonessa F, Foti D, Costa V, Chiefari E, Brunetti G, Leone F, Luciano F, Wu F, Lee AS, Gulletta E, Fusco A, Brunetti A. Activator protein-2 overexpression accounts for increased insulin receptor expression in human breast cancer. *Cancer Res.* 2006; **66**: 5085–5093.

33. Wei L, Hubbard SR, Hendrickson WA, Ellis L. Expression, characterization, and crystallization of the catalytic core of the human insulin receptor protein-tyrosine kinase domain. *J. Biol. Chem.* 1995; **270**: 8122–8130.

34. Songyang Z, Carraway KL III, Eck MJ, Harrison SC, Feldman RA, Mohammadi M, Schlessinger J, Hubbard SR, Smith DP, Eng C, Lorenzo MJ, Ponder BAJ, Mayer BJ, Cantley LC. Catalytic specificity of protein-tyrosine kinases is critical for selective signalling. *Nature* 1995; **373**: 536–539.

35. Niv MY, Rubin H, Cohen J, Tsirulnikov L, Licht T, Peretzman-Shemer A, Cna'an E, Tartakovsky A, Stein I, Albeck S, Weinstein I, Goldenberg-Furmanov M, Tobi D, Cohen E, Laster M, Ben-Sasson SA, Reuveni H. Sequence-based design of kinase inhibitors applicable for therapeutics and target identification. *J. Biol. Chem.* 2004; **279**: 1242–1255.

36. Abe M, Kuroda Y, Hirose M, Kato M, Murakami M, Watanabe Y, Nakano M, Handa T. Inhibition of autophosphorylation of epidermal growth factor receptor by a small peptide not employing an ATP-competitive mechanism. *Biopolymers* 2008; **89**: 40–51.

37. Levitzki A. Protein kinase inhibitors as a therapeutic modality. *Acc. Chem. Res.* 2003; **36**: 462–469.

38. Warren GL, Andrews CW, Capelli A-M, Clarke B, LaLonde J, Lambert MH, Lindvall M, Nevins N, Semus SF, Senger S, Tedesco G, Wall ID, Woolven JM, Peishoff CE, Head MS. A critical assessment of docking programs and scoring functions. *J. Med. Chem.* 2006; **49**: 5912–5931.

39. Levitzki A, Mishani E. Tyrphostins and other tyrosine kinase inhibitors. *Annu. Rev. Biochem.* 2006; **75**: 93–109.

40. Traut TW. Physiological concentrations of purines and pyrimidines. *Mol. Cell. Biochem.* 1994; 140: 1–22.

41. Lawrence DS, Niu J. Protein kinase inhibitors: the tyrosine-specific protein kinases. *Pharmacol. Ther.* 1998; **77**: 81–114.

LEGENDS OF FIGURES

Figure 1 Phosphorylation of purified IR in the presence or absence of (a) DIYET, (b) DYYRK, and (c) a mixture of DIYET and DYYRK. IR was incubated with or without peptides for 10 min at 37°C in buffer containing ATP. The concentration of ATP was 20 μM, 200 μM, or 2000 μM. Results displayed in the top panels represent typical immunoblots (IB). *P<0.05, **P<0.01 versus insulin-stimulated tyrosine phosphorylation at 10-min incubation without peptides; n = 3–4 for each lane.

Figure 2 Phosphorylation of purified IR in the presence or absence of peptides in which tyrosine residue is replaced with alanine, phenylalanine, or phosphotyrosine. The corresponding parent peptides are (a) DIYET and (b) DYYRK. IR was incubated with or without peptides for 10 min at 37°C in the buffer containing 20 μM of ATP. Results displayed in the top panels represent typical immunoblots (IB). *P<0.05, **P<0.01 versus insulin-stimulated tyrosine phosphorylation at 10-min incubation without peptides; n = 4 for each lane.

Figure 3 Phosphorylation of purified IR in the presence or absence of (a) NIYQT or (b) NYYRK. IR was incubated with or without peptides for 10 min at 37°C in buffer containing ATP. The concentration of ATP was 20 μM, 200 μM, or 2000 μM. Results displayed in the top panels represent typical immunoblots (IB). *P<0.05, **P<0.01 versus insulin-stimulated tyrosine phosphorylation at 10 min incubation without peptides; #P<0.05 versus tyrosine phosphorylation at 20 μM ATP; n = 3 for each lane.

Figure 4 Phosphorylation of purified epidermal growth factor receptor (EGFR) in the presence or absence of (a) DIYET (white bars), DYYRK (shaded bars), NYYRK (black bars), or (b) NIYQT. IR was incubated for 10 min at 37°C in buffer containing 20 μM ATP. Results displayed in the top panels represent typical immunoblots (IB). *P<0.05, **P<0.01 versus EGF-stimulated tyrosine phosphorylation at 10-min incubation without inhibitors; n = 4 for each lane.

Figure 5 Mass spectra of the solutions for mixtures of DIYET and DYYRK incubated with IR, insulin, and ATP. The reaction mixture was desalted with the solid-phase extraction method. (a) Negative-ion mode mass spectrum of the eluent for DIYET (75% A, 25% B); (b) negative-ion mode mass spectrum of the eluent for DYYRK (80% A and 20 % B). A is 0.1% TFA in water and B is 0.1 % TFA in acetonitrile.

Figure 6 Schematic drawing of the initial position of a peptide for docking simulations and the

resulting locations (Site 1 and Site 2) of the peptide in IRK. The crucial regions described in the text are labeled. The initial position of all peptides was set as the substrate-binding site surrounded by αEF (Pro1178–Asp1183), αG (Asn1215–Met1223), β11 (Leu1170-Leu1171), P+1 loop (Leu1171-Ala1177), and the catalytic loop (His1130–Asn1137). Site 1 represents the ATP-binding region and Site 2 represents a region surrounded by αC (Leu1038–Met1051), the Gly-rich loop (Gly1003–Gly1008), and the catalytic loop.

Figure 7 Conformations of DIYET calculated using GRID score function. Ten conformations which have lower energy are overlaid as line models and the most stable conformation is colored in red. The backbone of IRK are displayed as a green line.

Figure 8 Proposed binding models of (a) DIYET, (b) DYYRK, (c) NIYQT, and (d) NYYRK for IRK calculated using AMBER score function. The backbone of IRK is displayed as a ribbon model in yellow and the side chains of catalytic Asp1132 and Arg1136 are displayed as stick models in blue. The peptides are displayed as stick models in green.

Table I Theoretical and observed *m/z* values for peptides in negative ion mass spectra

	Theoretical (monoisotope)		Observed	
	$[M–H]^-$	$[M–2H]^{2-}$	$[M–H]^-$	$[M–2H]^{2-}$
DIYET	679.29	339.14	N.D.	N.D.
DIpYET	759.26	379.13	N.D.	379.0
DYYRK	783.38	391.19	N.D.	N.D.
DpYYRK or DYpYRK	863.35	431.17	N.D.	N.D.
DpYpYRK	943.31	471.15	N.D.	471.0

N.D., Not detected

Table II Theoretical and observed *m/z* values for peptides in positive ion mass spectra

	Theoretical (monoisotope)		Observed	
	$[M+H]^+$	$[M+2H]^{2+}$	$[M+H]^+$	$[M+2H]^{2+}$
NIYQT	679.34	340.17	N.D.	340.0
NIpYQT	759.31	380.16	N.D.	380.2
NYYRK	784.41	392.70	N.D.	392.6
NpYYRK or NYpYRK	864.38	435.57	N.D.	N.D.
NpYpYRK	944.34	472.68	N.D.	N.D.

N.D., Not detected

Table III Occupancy of the conformation of each peptide which has the best score estimated according to the Boltzmann distribution

	The best score (J)	Boltzmann factor ($\exp(-\beta\varepsilon_i)$)	Partition function ($\Sigma_j \exp(-\beta\varepsilon_j)$)	Occupancy
DIYET	-5.437×10^{-19}	1.395×10^{55}	1.395×10^{55}	~1.000
DYYRK	-6.798×10^{-19}	8.729×10^{68}	8.731×10^{68}	0.9998
NIYQT	-5.185×10^{-19}	3.897×10^{52}	4.516×10^{52}	0.8629
NYYRK	-6.108×10^{-19}	8.910×10^{61}	8.910×10^{61}	~1.000

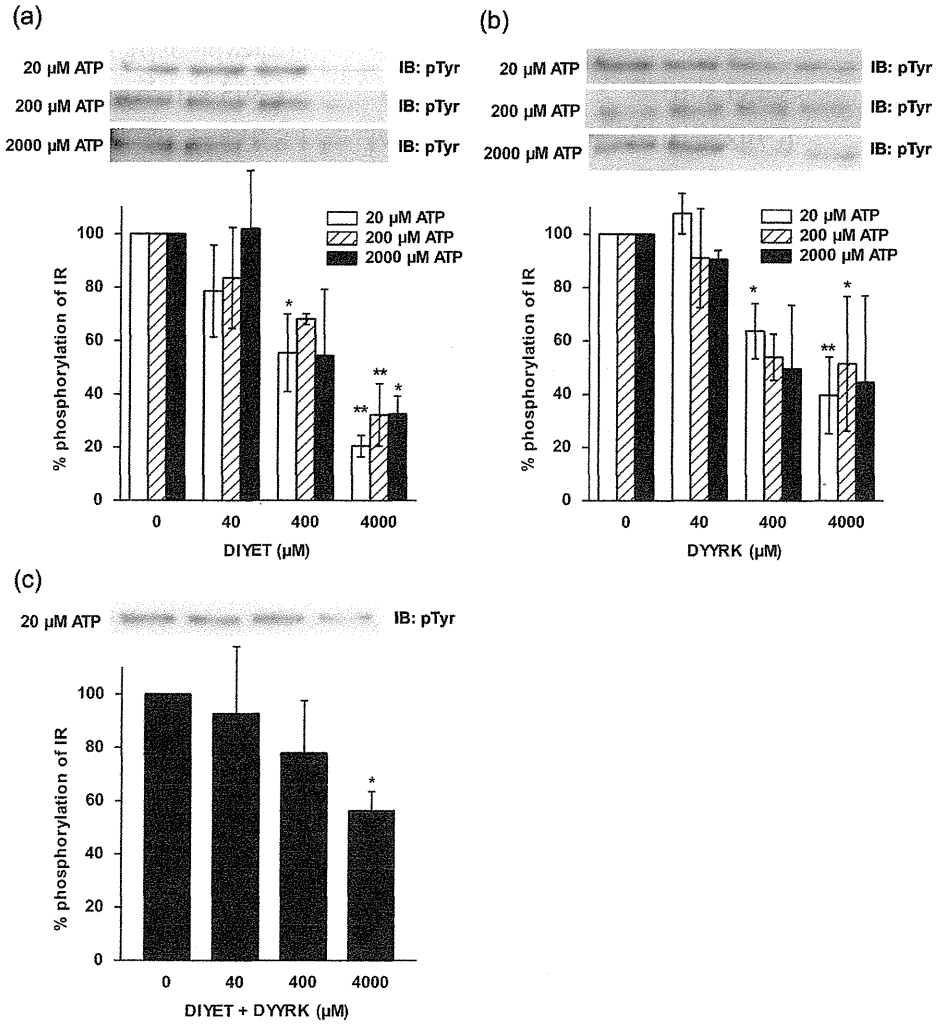

Figure 1 Phosphorylation of purified IR in the presence or absence of (a) DIYET, (b) DYYRK, and (c) a mixture of DIYET and DYYRK. IR was incubated with or without peptides for 10 min at 37°C in buffer containing ATP. The concentration of ATP was 20 microM, 200 microM, or 2000 microM. Results displayed in the top panels represent typical immunoblots (IB). *P<0.05, **P<0.01 versus insulin-stimulated tyrosine phosphorylation at 10-min incubation without peptides; n = 3□4 for each lane.
160x180mm (600 x 600 DPI)

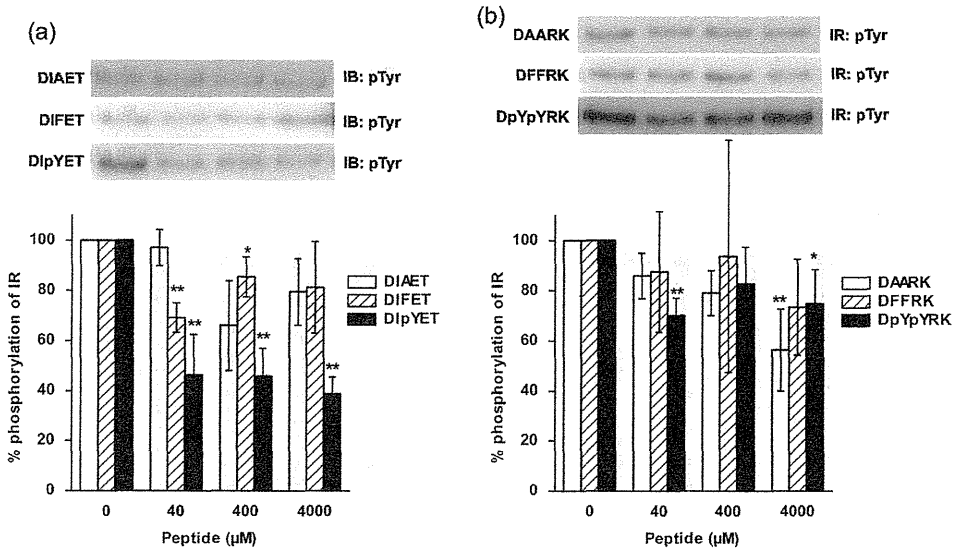

Figure 2 Phosphorylation of purified IR in the presence or absence of peptides in which tyrosine residue is replaced with alanine, phenylalanine, or phosphotyrosine. The corresponding parent peptides are (a) DIYET and (b) DYYRK. IR was incubated with or without peptides for 10 min at 37°C in the buffer containing 20 microM of ATP. Results displayed in the top panels represent typical immunoblots (IB). *P<0.05, **P<0.01 versus insulin-stimulated tyrosine phosphorylation at 10-min incubation without peptides; n = 4 for each lane.
170x99mm (600 x 600 DPI)

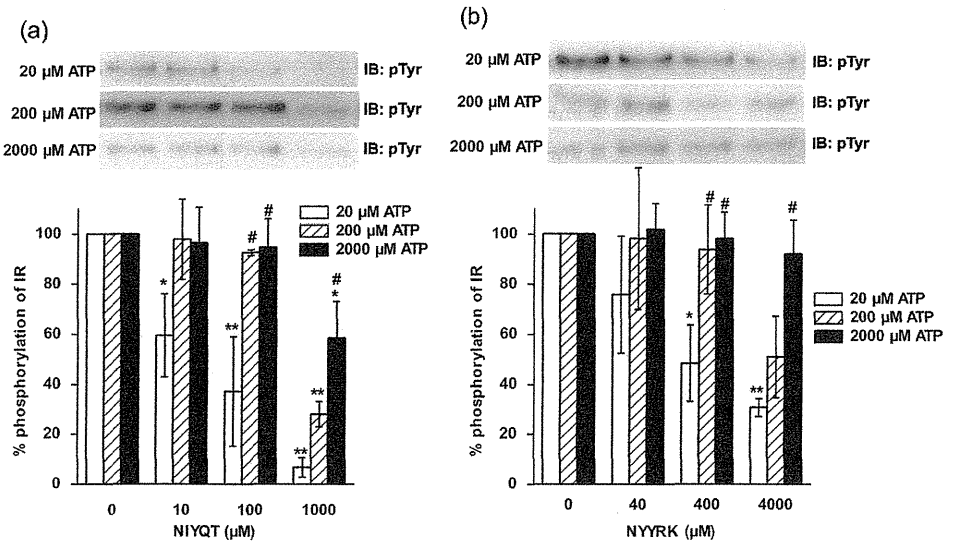

Figure 3 Phosphorylation of purified IR in the presence or absence of (a) NIYQT or (b) NYYRK. IR was incubated with or without peptides for 10 min at 37°C in buffer containing ATP. The concentration of ATP was 20 microM, 200 microM, or 2000 microM. Results displayed in the top panels represent typical immunoblots (IB). *P<0.05, **P<0.01 versus insulin-stimulated tyrosine phosphorylation at 10 min incubation without peptides; #P<0.05 versus tyrosine phosphorylation at 20 microM ATP; n = 3 for each lane.
170x99mm (600 x 600 DPI)

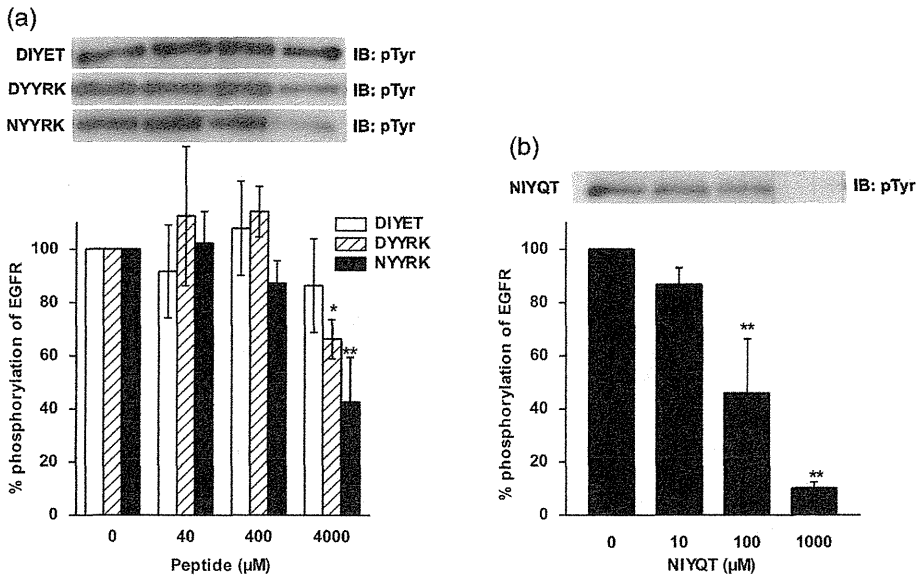

Figure 4 Phosphorylation of purified epidermal growth factor receptor (EGFR) in the presence or absence of (a) DIYET (white bars), DYYRK (shaded bars), NYYRK (black bars), or (b) NIYQT. IR was incubated for 10 min at 37°C in buffer containing 20 microM ATP. Results displayed in the top panels represent typical immunoblots (IB). *P<0.05, **P<0.01 versus EGF-stimulated tyrosine phosphorylation at 10-min incubation without inhibitors; n = 4 for each lane.
160x99mm (600 x 600 DPI)

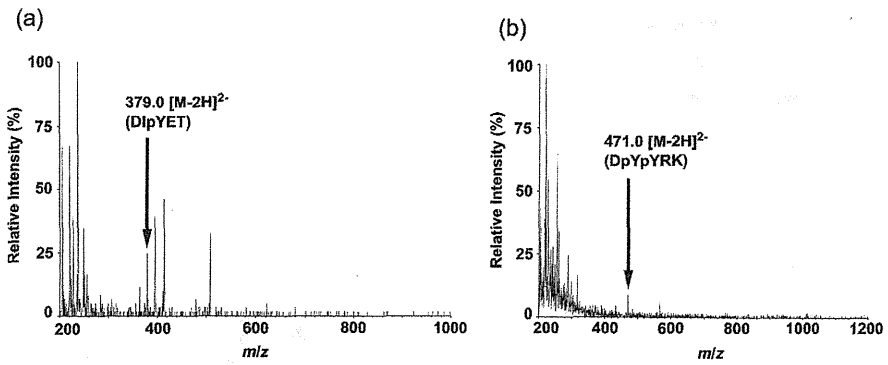

Figure 5 Mass spectra of the solutions for mixtures of DIYET and DYYRK incubated with IR, insulin, and ATP. The reaction mixture was desalted with the solid-phase extraction method. (a) Negative-ion mode mass spectrum of the eluent for DIYET (75% A, 25% B); (b) negative-ion mode mass spectrum of the eluent for DYYRK (80% A and 20 % B). A is 0.1% TFA in water and B is 0.1 % TFA in acetonitrile.
170x75mm (600 x 600 DPI)

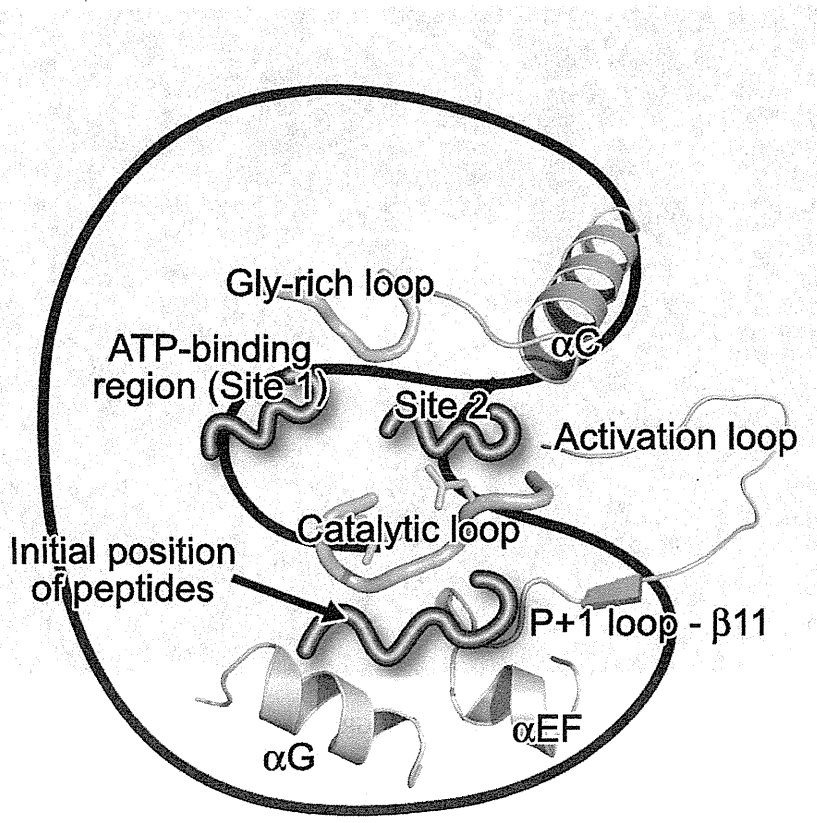

Figure 6 Schematic drawing of the initial position of a peptide for docking simulations and the resulting locations (Site 1 and Site 2) of the peptide in IRK. The crucial regions described in the text are labeled. The initial position of all peptides was set as the substrate-binding site surrounded by alphaEF (Pro1178-Asp1183), alphaG (Asn1215-Met1223), beta11 (Leu1170-Leu1171), P+1 loop (Leu1171-Ala1177), and the catalytic loop (His1130-Asn1137). Site 1 represents the ATP-binding region and Site 2 represents a region surrounded by alphaC (Leu1038-Met1051), the Gly-rich loop (Gly1003-Gly1008), and the catalytic loop.
80x80mm (600 x 600 DPI)

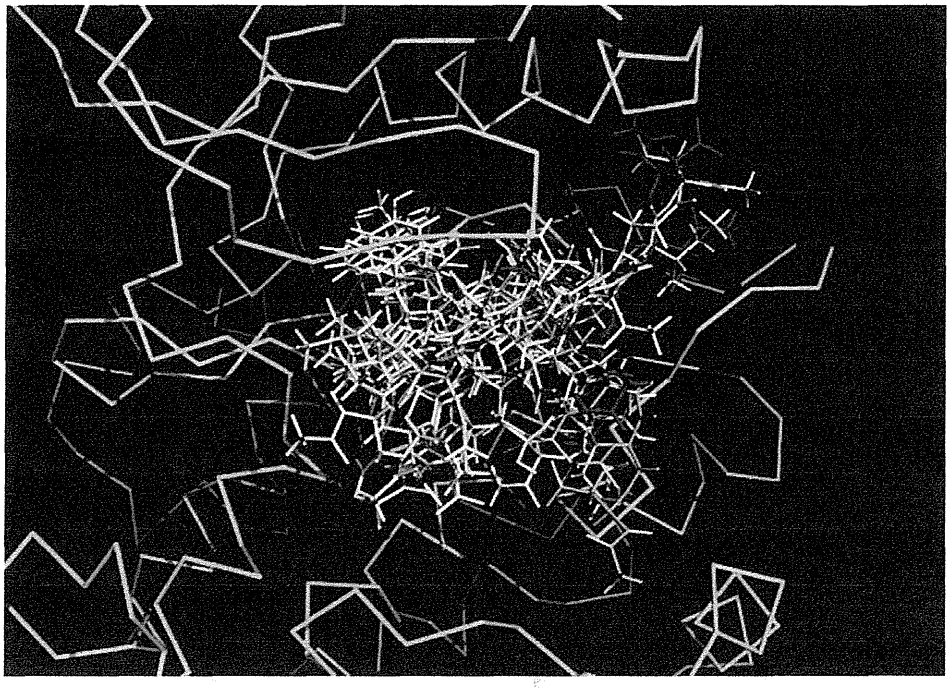

Figure 7 Conformations of DIYET calculated using GRID score function. Ten conformations which have lower energy are overlaid as line models and the most stable conformation is colored in red. The backbone of IRK are displayed as a green line.
70x50mm (600 x 600 DPI)

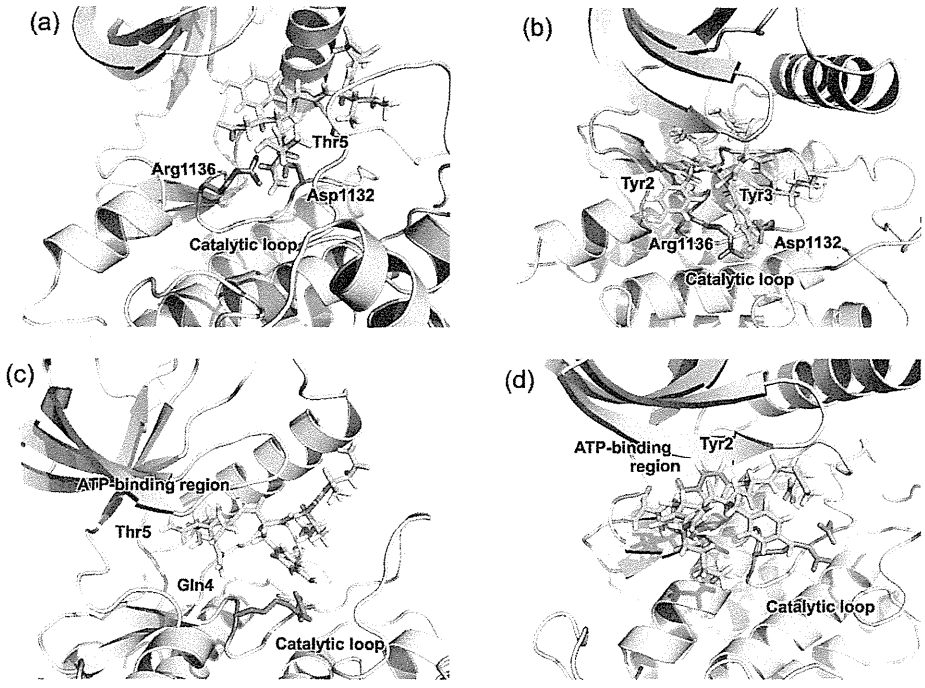

Figure 8 Proposed binding models of (a) DIYET, (b) DYYRK, (c) NIYQT, and (d) NYYRK for IRK calculated using AMBER score function. The backbone of IRK is displayed as a ribbon model in yellow and the side chains of catalytic Asp1132 and Arg1136 are displayed as stick models in blue. The peptides are displayed as stick models in green.
160x119mm (600 x 600 DPI)

SHORT ABSTRACT

In an attempt to develop non-ATP-competitive inhibitors of the autophosphorylation of insulin receptor (IR), the effects of the pentapeptides, Ac-DIYET-NH_2 and Ac-DYYRK-NH_2, on the phosphorylation of IR were studied. The peptides were derived from the amino-acid sequence in the activation loop of IR. The peptides inhibited the autophosphorylation of IR in a non-ATP-competitive manner. Mass spectrometry and simulations showed that the peptides would interact with the catalytic loop of IR. Thus, these peptides are expected to be non-ATP-competitive inhibitors.

Int. J. Environ. Res. Public Health **2009**, *6*, 3056-3069; doi:10.3390/ijerph6123056

OPEN ACCESS

International Journal of
Environmental Research and Public Health
ISSN 1660-4601
www.mdpi.com/journal/ijerph

Article

Assessment of Japanese Stimulant Control Law Offenders Using the Addiction Severity Index—Japanese Version: Comparison with Patients in Treatment Settings

Takashi Watanabe [1,2,#], Yasukazu Ogai [3,#], Takehiro Koga [2], Eiichi Senoo [4], Kazuhiko Nakamura [1], Norio Mori [1] and Kazutaka Ikeda [3,*]

[1] Hamamatsu University School of Medicine, 1-20-1 Handayama, Higashi-ku, Hamamatsu, Japan; E-Mails: takashi_matuki@yahoo.co.jp (T.W.); nakamura@hama-med.ac.jp (K.N.); morin@hama-med.ac.jp (N.M.)

[2] Shizuoka Prison, 3-1-1 Higashichiyoda, Aoi-ku, Shizuoka, Japan; E-Mail: kg-ronnie@fmwbs.jp

[3] Division of Psychobiology, Tokyo Institute of Psychiatry, 2-1-8 Kamikitazawa, Setagaya-ku, Tokyo 156-8585, Japan; E-Mail: y-oogai@prit.go.jp

[4] Division of Social Psychiatry, Tokyo Institute of Psychiatry, 2-1-8 Kamikitazawa, Setagaya-ku, Tokyo 156-8585, Japan; E-Mail: senoo@prit.go.jp

[#] These authors contributed equally to this study.

* Author to whom correspondence should be addressed; E-Mail: ikedak@prit.go.jp; Tel: +81-3-3304-5701 ext. 508; Fax: +81-3-3329-8035.

Received: 9 November 2009 / Accepted: 29 November 2009 / Published: 3 December 2009

Abstract: The present study assessed problems in Japanese prisoners (inmates) who abused methamphetamine. Fifty-two male inmates were assessed in 2005–2007 using the Addiction Severity Index-Japanese version and compared with 55 male methamphetamine abusers in hospitals and recovery centers. The χ^2 and Mann-Whitney-Wilcoxon tests showed that the inmates had a significantly lower education level, more frequently had full-time jobs, had more experience living with a sexual partner, and more frequently had a history of juvenile delinquency and criminal records than patients. Although psychiatric symptoms, such as depression, anxiety, and hallucinations, were not common among inmates, suicidal behavior and trouble controlling violence were common in both groups.

Keywords: methamphetamine; Addiction Severity Index; Japanese; prison; correctional facilities

1. Introduction

The production, trafficking, and use of amphetamine-type stimulants have increased significantly since the 1990s throughout East Asia and the Pacific countries [1]. The most prevalent amphetamine-type stimulant in East Asia is methamphetamine, the principal drug involved in drug abuse cases in Japan [2,3]. Stimulant dependence presents a serious problem, not only for patients, but also for Japanese society [4]. For example, about 25% of convicted prisoners committed offenses under the Stimulant Control Law [5]. Although many Japanese methamphetamine abusers have received only punishment rather than medical treatment [3], drug-abuse problems in inmates have not been sufficiently investigated. Moreover, appropriate assessment and treatment of substance abuse have not been provided in Japanese prisons, partly because the number of inmates in Japan exceeds prison capacity.

In a study conducted at a Japanese hospital, methamphetamine abusers with serious criminal records tended to administer the drug by injection and had less chronic psychosis than those with less serious criminal records [6]. In a study of adolescents at a juvenile detention home, Miura *et al.* [7] reported that gender (female), age, number of admissions, violence, history of psychiatric treatment, and family history of drug misuse were significantly associated with methamphetamine use. Matsumoto *et al.* [8] reported no significant correlation between drug abuse and antisocial behaviors in male juvenile delinquents, although alcohol abuse has been hypothesized to promote these behaviors. The aforementioned studies, however, did not include Japanese inmates under the Stimulant Control Law in their sample. Although Matsumoto *et al.* [9] found a relationship between childhood tendencies toward attention-deficit/hyperactivity disorder and illicit drug abuse in Japanese prisoners, they did not compare the characteristics of methamphetamine abusers in prison with those in treatment facilities. Investigation of methamphetamine abusers in correctional settings and comparison of the results with those in treatment settings would elucidate the specific characteristics of methamphetamine abusers in correctional settings.

The Addiction Severity Index (ASI) [10] is used worldwide and is one of the few standardized instruments that address drug abuse. The ASI assesses legal status in addition to medical status, employment/support status, drug use status, alcohol use status, family/social status, and psychiatric status. These features make the ASI particularly useful for practitioners working with substance-abusing offenders [11]. For example, some studies used the ASI with inmates to confirm their common characteristics [12], to compare inmates with other drug abusers [10], and to confirm the effectiveness of the ASI as a screening tool for substance use disorders [13]. The ASI was also used to examine associations between psychosocial and criminal factors [14], relationships between prescription drug abuse and addiction severity [15], gender differences in substance abuse disorders [16], the effectiveness of methadone maintenance treatment [17], and the predictors of treatment motivation [18]. The

ASI-Japanese version (ASI-J) has acceptable reliability and validity for Japanese drug abusers in treatment settings [19].

Using the ASI-J, the present study assessed the characteristics and problems of Japanese inmates who abuse methamphetamine by comparing them with methamphetamine-abusing patients in treatment settings. Revealing such characteristics and problems may contribute to improving substance abuse treatment policy and improving the effectiveness of interventions designed to reduce stimulant abuse and its adverse consequences.

2. Methods

2.1. Recruitment Site

The participants were recruited from an adult male-only prison in Shizuoka, Japan, from September 2005 to July 2006 and in February 2007. In this prison, offenders mainly came from Tokyo or Shizuoka prefectures. In cases of repeat offenders, the inmates were detained in this prison for the first three months of their sentence. In October 2005, for example, 178 (164 Japanese and 14 foreigners) of the 1,407 total inmates were imprisoned for methamphetamine use as a result of the Stimulant Control Law.

2.2. Participants and Procedure

The study was approved by the Institutional Review Board of each facility. Sixty-three Japanese adult (>20 years old) male inmates who were arrested for methamphetamine use based on the Stimulant Control Law were sequentially approached to participate in this study. They were recruited and interviewed within three months after their imprisonment. Of the 63 inmates, five (7.9%) refused to participate, and the remaining 58 (92.1%) were administered the Structured Clinical Interview of the *Diagnostic and Statistical Manual of Mental Disorders*, 4th edition (DSM-IV) [20], Substance Abuse Disorders module. After the interview, five (7.9%) inmates were excluded from the study because they were not diagnosed with substance abuse or dependence. Written informed consent was obtained from the remaining 53 (84.0%) inmates. No inmates presented with acute psychosis.

The ASI-J was administered to the 53 inmates to assess their characteristics and the severity of their problems. They were asked about their status before they had been arrested by the police. One inmate was excluded because of a pathologically disorganized response. Thus, data from 52 (82.5%) inmates were included in the statistical analysis.

One psychiatrist and two clinical psychologists recruited participants and interviewed them. To achieve inter-rater reliability, two interviewers received six sessions of training interviews with another expert interviewer to confirm rating consensus between all interviewers. Each interview for each participant took approximately 60 min to complete.